

An air-polymer analogy for modeling air flow through rubber-metal interface

Gilad Pagi, Eli Altus
Faculty of Mechanical Engineering
Technion – Israel Institute of Technology
Haifa, 32000
ISRAEL
Email: gilad@tx.technion.ac.il

Abstract: - A system composed of a metallic cylinder, filled with pressured air (up to 5 atm), and a rubber, square sectioned ring seal, was investigated theoretically and experimentally. Under a certain pressure difference (p) (internal minus atmosphere) and external sealing force, the rubber seal is compressed (h) and should prevent air leakage. In a certain p range, a continuous, nonlinear decrease in $p(t)$ as a function of time is detected. A few classical (macro) thermodynamic models for predicting $p(t)$, by considering air flow through cracks, have been suggested before [1], but they have failed to describe the profile in question due to the coupled constitutive properties of rubber and a construction that allow the creation of micro-scale "tunnels" in the rubber-lid interface, through which the air can pass. A novel heuristic model, which assumes an analogy between the micro-scale air streamlines and polymer strands is proposed. Thus, polymer equations based on statistical thermodynamics are applied on the air streamlines. Using this model, there are four unset parameters whose values are being determined by the experimental profiles, similar to the semi-phenomenological rubber model of Mooney-Rivlin. An excellent correspondence between the model and the experimental data is achieved, which suggests that the model captures some physical essence of the phenomenon. Many standard trend-lines have been tested and failed to describe $p(t)$ accurately, including 3rd order polynomial which has also four parameters.

Key-Words: - Sealing, Pressure drop, Air leakage, Air-Polymer analogy, Polym-Air, Micro-Macro, Langevin.

1 Introduction

An air pressure metal cylinder (up to 5atm) is covered and sealed with a rubber, square sectioned ring, as seen in [1]. Under a certain pressure difference (internal minus atmosphere pressure - p) and external sealing force, the rubber seal is compressed (h) and should prevent air leakage. However, experiments show a continuous, nonlinear decrease in p as a function of time.

A few classical (macro) thermodynamic models for predicting $p(t)$, by describing air flow through cracks (of heat regenerator for example) have been previously suggested ([2]) but they have failed to accurately describe the profile in the following specific setup due to the coupled constitutive property of rubber and a construction that allows the creation of micro-scale "tunnels" in the rubber-lid interface, through which the air can pass. Several mathematical and physical models of describing air flow through cracks are available in [3], [4], but those have to be adjusted to describe air flow through rubber-metal interface. Moreover a simple control volume analysis is insufficient.

Background knowledge in statistical thermodynamics and rubber thermodynamics is

essential for constructing the model described in the following sections. This article will be based on some results and the jargon of [5]-[9]. An equation of great importance is (13-13) in [8] stating for a freely joint polymer strand

$$\tau = \frac{kT}{a} \mathcal{L}^{-1} \left(\frac{\bar{l}}{Ma} \right) \quad (1)$$
$$\mathcal{L}(x) = -\frac{1}{x} + \coth(x),$$

where τ is the tensile force acting on the polymer, M is the number of monomers, a is Kuhn length, kT is the multiplication of Boltzmann constant by the temperature and l is the projected length. Bar superscript represents time average or space average (which are equal by the Ergodic Assumption). \mathcal{L} is the Langevin function and \mathcal{L}^{-1} is its inverse. (1) is valid as long as the argument in \mathcal{L}^{-1} is between 0 and 1.

In the following, we will describe the construct classical and modern models to predict the analytical form of the pressure profile. Finally we will compare to experimental results. We shall see that due to lack of relations between the different parameters, the proposed model becomes semi-

phenomenological. The uncertainty of the influence of the air-rubber interaction on the flow rate is represented in [10].

2 Experiment Setup

2.1 Introduction and Targets

Full details regarding the experiment can be found in [1]. We shall use some notions and results presented there.

Consider the setup where the inner pressure is set to a constant value, which is different from the atmospheric pressure as described in [1]. The "Force" preventing from the piston to pop up and also causes the rubber seal to be subjected to uniaxial compression. Thus, the vertical length – originally h_0 – decreases to a controlled value h . Once deformed enough, the seal prevents leakage of air from the inside. Note that thanks to the upper airway the outer surface of the seal is subjected to P_a .

The main target is to investigate the pressure vs. time $p(t)$ profile. The seal's function, is to preserve the pressure difference $p=P-P_a$ between the two gasket sides. The mechanism of air leakage through the seal at poor sealing is also presented in [1].

2.2 Preliminary results and Conclusions

$p(t)$ profile was recorded for different initial pressure difference and rubber deformations. The parameters range are: $p_0=1-5[atm]$, $\varepsilon=(h_0-h)/h_0=0$ to -0.2 .

Preliminary results showed that $p(t)$ graphs were different considerably one from the other for the same initial conditions. It was concluded that the experiment is very sensitive to the rubber gaskets specimen, that is, a property that varies over the specimen i.e., surface quality. See fig.1 for more details.

To check this assumption, few experiments were conducted with the same gasket, and it was shown [1] that the repeatability was much higher.

3 Theoretical Modeling

3.1 Qualitative Chain of Actions

The proposed micromechanical model of leakage is based on three phases.

Phase I includes placing the rubber gasket and deforming it to the set value h .

The polymer microstructure is composed of strands and junctions. According to the non-entangled mechanical models [6], the junctions (at least, the ones on the surface) move affinely due to compression and each strand remain attached to its

original junctions. The junctions and strand getting closer and dense in the bulk of the rubber gasket (which were dense enough already to prevent air flow). However, the surface isn't a mosaic of junctions but more of a blend of junctions and loose strands – strands connected only to one junction – creating coarse surface profile. We get a flow through the rubber-metal interface where the topology (can be seen in the top view - fig. 2) is pressure dependent: as the pressure difference decays, the streamlines become curvier. See [1] for more details.

Phase II is the pressure buildup. We open the main valve, letting air to flow from the supply line to the cylinder. The supply line pressure is controlled and thus raising the pressure inside the cylinder. At this phase, air is pumped in and leaks out at the same time but the influx rate is much greater than the leakage rate. When the level of pressure reaches the desired one, and stables, the secondary valve is closed and phase III is being executed.

In phase III, the air flows out through the interface between the seal and the metal lid. Let's take a top view (fig. 2) on one of the two interface planes and examine how the air finds its way out, or how the streamlines are arranged.

The air doesn't search for the shortest way out but for the less "energetic". The path choosing requires a trade-off between the friction loss and the path potential energy. The minimum energy principle sets the relation between the pressure difference and the paths' topology stated before and in [1]. Therefore the streamline arrangement changes with pressure, and its topology isn't constant. In addition, the streamline morphology can change from one sample to the other, including the number of streamlines, due to different surface profiles.

Through those micro-airways, the air sneaks out and causes pressure drop. The phase, and the experiment, ends when the pressure difference is small enough, so there's no conventional airflow but rather an exit of air in "percolation". Reaching that

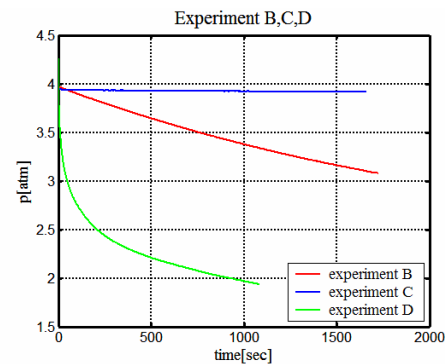


Figure 1 – Three pressure profiles for specimens B,C,D. $p_0 \approx 4.1[atm]$, $\varepsilon \approx 0.148$.

region, the pressure drop rate is too small and the experiment ends there. In this study, we are only interested in the poor sealing region, where the air exits by continuous streamlines.

Another important observation shown in [1] (see discussion and videotaped experiment) is that rubber ring expands during the first phase and doesn't contract until the middle of phase III. Meaning in phase III there are two regions where the volume within the rubber seal remains constant. It is also possible for the rubber not to contract at all (the two regions coincide).

3.2 Classical Model - Bernoulli's Streamline

Let's observe figure 2 again. It might be possible that a streamline ends inside the rubber plane and never reaches outside. We ignore this kind of streamlines and therefore count the number of streamlines as the number of those that end outside and denote it as N_l . In case that several lines are joined together, we will count them separately. In order to use Bernoulli's equation, one should assure steady state incompressible frictionless flow. This is clearly not the case, since the inner pressure drops constantly and the air velocity might change from one kind of rubber to the other due to friction between the air molecules and the loose strands. Moreover, each streamline is microscopic and macroscopic analysis can unintentionally neglect important phenomena for the micro case. Nevertheless, it is a good start for modeling phase III which is our main concern.

Assuming an ideal gas, we have

$$P_{ab} = \frac{M}{V} RT = \rho RT \quad (2)$$

P_{ab} denotes the absolute pressure, M the mass, V the volume and ρ the density. Now, we would like to use Bernoulli's equation between a point in the inner volume to a point at the exit of a streamline. We neglect gravitational effects and the entrance

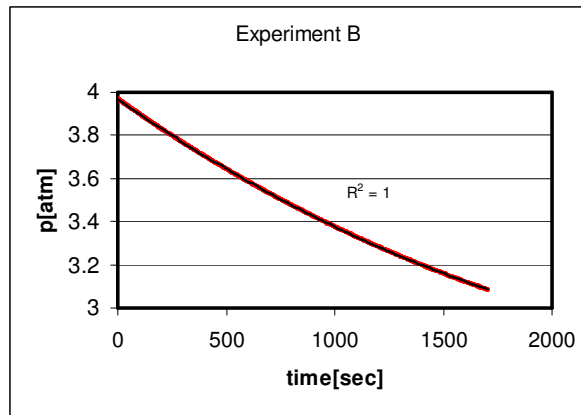


Figure 3 - 2nd order polynomial trendline in black, describing the actual profile in red for sample B.

velocity, leading to:

$$P_{ab,in} = P_a + \rho_a \frac{v^2}{2} \quad (3)$$

$$\Rightarrow p = \frac{P_a}{RT} \frac{v^2}{2} \Rightarrow v = \sqrt{\frac{2RTp}{P_a}}$$

Further, we examine the mass conservation equation and continuing the discussion by assuming isothermal process and using the equations we have so far.

$$\left[\frac{\partial(\rho V)}{\partial t} \right]_{in} = \dot{M}_{in} = N_l \rho_a A v$$

$$\Rightarrow \dot{\rho}_{in} V + \rho_{in} \dot{V} = N_l \rho_a A \sqrt{\frac{2RTp}{P_a}} \quad (4)$$

$$\left(\dot{\rho}_{in} = \frac{\dot{P}_{ab,in}}{RT} = \frac{\dot{p}}{RT} \Rightarrow \right)$$

$$\Rightarrow \dot{p} V + p \dot{V} = N_l p_a A \sqrt{\frac{2RTp}{P_a}}$$

A is a typical section area of a streamline. If the change of volume is negligible we obtain:

$$\dot{p} V = N_l p_a A \sqrt{\frac{2RTp}{P_a}} \Rightarrow \frac{\dot{p}}{\sqrt{p}} = \tilde{C} \Rightarrow \sqrt{p} = Ct + D \quad (5)$$

$$\Rightarrow p = (Ct + D)^2; p(t=0) = p_0; C > 0.$$

A calculation with the given dimensions and considering and the experimentally found rubber expansion show that the change of the volume is absolutely not negligible.

In spite of the above crude assumptions, it is very surprising to see that in some experiments the 2nd order polynomial trendline fits almost perfectly (fig.3). Note that the samples were denoted A,B,C etc. Full results will be presented in the last chapter.

In other samples, Bernoulli model produces fine correspondences at the beginning and the end of the profile, but fails to describe the whole process.

3.3 The "Polym-air" model

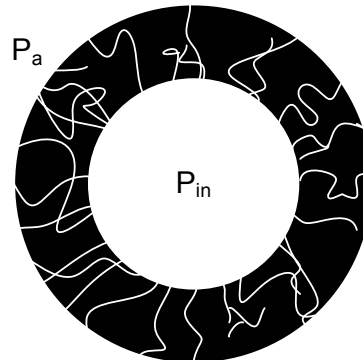


Figure 2 - schematic drawing of the steamlines

3.3.1 Introduction and Motivation

Upon examining figure 2, it is realized that the streamline arrangements look similar to an ensemble of air strands filling the hollows between the rubber strands. It's tempting to treat the 2D streamlines as a 2D polymer. Moreover, we preserve the "streamline-strand" analogy basing on a one-to-one mapping of streamlines to strands. In case of two or more streamlines connected before the exit we look at them as two or more strands placed one under the other. Thus, the one-to-one mapping is achieved.

We would like to refer to a single streamline as a one strand of polymer and apply equation (1). The tension is analogous to the pressure difference as they both tend to straighten the polymer/streamline. The correspondence is through the relation:

$$\tau \leftrightarrow Ap. \quad (6)$$

This analogy arises from the similarity between the "tension-strand topology relations" and "pressure-air topology relations" introduced above.

Moreover, the strand is made from M monomers with uniform length a . When the pressure difference is zero, the air is free to go in each direction with no restrictions or any influence of one monomer to the other so the polym-air is considered freely joint. When internal pressure is applied we can use (1) on the streamline ("chain with free joints" [7]).

Note the symmetry of the analogy. We took the air between the hollows of the polymers and switched roles – now, the polymer is filling the air hollows and the system obeys the same rules. Of course, the polymer must be dense enough and subjected to sufficient pressure in order to achieve polymer-like-topology of the air.

3.3.2 Basic Relations and Assumptions

Let's redefine the streamlines using polymer jargon. Recall that we ignore a line whose end-to-end vector's head is still in the polymer. Those do not contribute to the pressure leakage and can be treated as a rather negligible part of the inside volume that the air is filling during the experiment. We observe the streamlines that have an end-to-end vector with head positioned outside of the rubber gasket, and try to describe the air flow through the gasket-lid interface.

We consider a typical streamline as starting close to the inner radius of the gasket ($r_1 < R_m$) and ends close to the outer radius ($r_2 > R_{out}$). The M and a parameters are the geometric parameters since the polym-air is freely joint. Observe figure 4, given a hole in the inner lip of the gasket – a site for streamline creation. The direction of the x -axis is the vector connecting the center of the gasket and the

hole; that is due to the natural tendency of the streamline to align with this direction (minimum energy). In grey we can see three, out of infinite, possibilities of creating streamlines. Each streamline has its own starting point, end point and length l (along the x -axis). Theoretically, l has no limitations. If we denote the radii difference of the ring as δ ($D/2 - d/2 = \delta$), then l can be larger, smaller or equal to δ .

There is an assumption that almost must be made at this point:

$$\bar{l} = \delta. \quad (7)$$

If the pressure difference is not extremely large, the start and end points will be close to the surfaces of the gasket and then the lengths will be around δ in a somewhat narrow range. We now use equation (1) and create the most important relation (analogy) of this model:

$$Ap = \frac{kT}{a} \mathcal{L}^{-1} \left(\frac{\delta}{Ma} \right) \quad (8)$$

This equation describes the connection between the pressure difference and the topology of the streamlines. The next step is to set a connection between the topology of the streamlines and the pressure loss **rate**. Clearly, the air velocity is reduced when the streamline path is more curved, i.e., a smaller a . For simplicity we assume for a single streamline:

$$v = \alpha a, \quad (9)$$

where v is the velocity. The physical interpretation of (9) is somewhere between friction, surface quality and rubber-fluid interaction (see [10] for more details about fluid-surface interaction).

Let's summarize the main variables in the discussion:

1. kT - we assume that the temperature doesn't change, as we did before.
2. M - the number of monomers in a streamline changes stochastically during phase III of the experiment. The range of values is the natural numbers, and tends to increase as p decreases. Alternately, when p aspires to infinite the streamline would penetrate the rubber along the x -axis, making a long straight monomer (polym-air), so M aspires

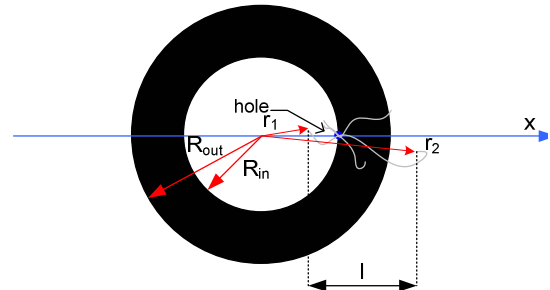


Figure 4 - streamline possibilities

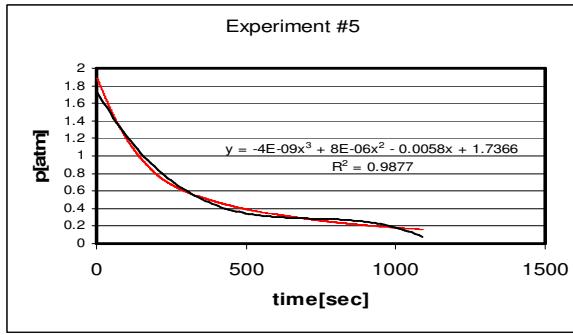


Figure 5 - best fit 3rd order polynomial

(as a distribution) to a constant 1.

3. a - the length of each monomer, which is inversely monotone with p from the same considerations for M .

4. δ - it is a mechanical parameter that supposed to capture the volume change also. During phase III, δ is a constant at the beginning of the process, but after some time it starts to increase and aspires to the initial dimensions of the rubber ring. This means that the pressure profile depends on δ through the mechanical model of the rubber. The typical cross section area A (maybe projected) of the streamline is another mechanical parameter that depends mainly on ε stochastically.

6. N_l - the number of streamlines is a monotonic random function of p , (stochastic in time). At the same time, as ε grows in magnitude, the number of streamlines decreases.

For a first order approximation we use the center limit theorem and assume that all the streamlines are statistically homogenous over time with narrow distribution, that is, "Act the same averagely". We now use equation (8) and replace each variant by its average.

Combining (6) with the statistical homogenous assumption, we can generalize (4):

$$\dot{p}V + p\dot{V} = N_l p_a A \alpha a. \quad (10)$$

In principle, one can rewrite the air volume using geometric parameters and finally, given a mechanical and metal-rubber friction model one should connect the volume change with (8) and (10) to obtain a first order ODE with the proper initial condition. Even if we had a good mechanical model in our toolbox, it would be difficult to predict precisely $p(t)$ since there are other variables whose numerical values are unknown, such as N_l , α .

3.4 Assuming Profiles

The first expression to be dealt with is δ/Ma , which is the ratio between the average projected length and the actual length of a typical air tunnel. This expression is the argument of the inverse Langevin function so it should be between 0 and 1. It is clear that higher pressure leads to shorter paths, so an

"exponential decay" profile seems to be a good candidate, which is also characteristic to linear viscoelastic processes.

Aa is the other expression to be assumed in (8). Considering (10), recall that at the beginning and the end of phase III the volume V doesn't change, and p is quadric due to Bernoulli's model. Therefore the expression Aa is close to be linear (if N_l doesn't interrupt), i.e.

$$Aa = (Zt - W)^2, \quad (11)$$

when Z is very small, $W > 0$, and the null point $t = W/Z$ occurs much after the final time of the experiment.

In the following chapter we shall see how this model, now a four-parameters-semi-phenomenological one, describes accurately 15 different experiments.

3.5 Final Outcome

Based on the final outcome:

$$p = (Zt - W)^{-2} \mathcal{L}^{-1}(Ce^{-rt}) \quad (12)$$

and given $p(t)$ data, the calculation process is:

1. Assume Z and W and multiply p by the relevant expression.
2. Apply Langevin function.
3. Apply exponential regression. Review the R^2 .

Thus, iteratively and based on some educational guesses, one can find the best values of the parameters Z, W, C, r .

4 Comparison with Experiments

4.1 Theoretical vs. Experiments

Using the method described above, 4 parameters were calculated for each experiment of the total of 15. The R^2 ranged from 0.99565 to 1.00000. See results in fig.6 for 3 experiments (chosen for visibility). In two out of the first 5 experiments, anomalies were detected at the initial stage (100 seconds out of 1000 - See discussion for details). For those two, the parameters were recalculated ignoring the first 100 seconds. Then the minimal R^2 improved to 0.99965. The average R^2 is 0.99992. Note that the model enables extrapolation. It is presented in fig. 6 but we shall not go into details about it.

For comparison, a best fit 3rd order polynomial (4 parameters) for one of the experiments was chosen for demonstration. The weak correspondence and "wavy" behavior which is not possible in a real profile is clearly seen (fig. 5). Another 4 parameter function, constructed from a sum of two exponents,

was applied and showed better graphical correspondence than the polynomial trend-line but was inferior to the proposed model.

4.2 Discussion

The proposed model can explain the differences in experimental results during the first stage of phase III. It is crucial to build the pressure from zero to the desired value, wait for stabilization – which is actually when the rubber stops its expansion - and then close the main valve and start monitoring. When the pressure is high, streamlines that are associated with high pressure are created. It is possible that after we decrease the pressure manually, they will stay with their high pressure properties because they have already managed to overcome the relevant obstacles. Such irreversibility, which was observed in two of the experiments, cannot be directly predicted by the model.

5 Conclusions

In this work we've seen that the air is leaking through the deformed rubber gasket in a decaying profile. Using a polymer-air analogy, we've constructed two models: classical and modified. The classical one gave a partial description, while the modified one provided excellent correspondence to experimental results, using the 4-parameter-semi-phenomenological profile.

Further work should be done in finding the source of the high sensitivity of the pressure profile to the initial conditions and the surface quality.

References:

- [1] <http://meeng.technion.ac.il/Research/TRreports/2007/ETR-2007-02.html>
- [2] T. Skeipko, R.K. Shah, Modeling and effect of leakages on heat transfer performance of fixed matrix regenerators, *International Journal of Heat and Mass Transfer*, No.48, 2005, pp. 1608–1632.
- [3] S.B.M. Beck, N.M. Bagshaw, J.R. Yates, Explicit equations for leak rates through narrow cracks, *International Journal of Pressure Vessels and Piping*, No.82, 2005, pp. 565–570.
- [4] L. Cizelj, G. Roussel, Probabilistic evaluation of leak rates through multiple defects: the case of nuclear steam generators, *Fatigue & Fracture of Engineering Material & Structures*, Vol.11, No.26, 2003, pp. 1069-1079, 2003.
- [5] M. Rubinstein, R.H. Colby, *polymer Physics*, Oxford, 2003.
- [6] S.L. Rosen, *Fundamental Principles of Polymeric Materials*, 2nd ed., John Wiley & sons, 1993.
- [7] B. Erman, J.E. Mark, *Structures and Properties of Rubberlike Networks*, Oxford, 1997
- [8] T.L. Hill, *An introduction to Statistical Thermodynamics*, Dover, 1986.
- [9] P.J. Flory, *statistical mechanics of chain molecules*, Hanser, 1989.
- [10] Chivers TC, The influence of surface roughness on fluid flow through cracks, *Fatigue & Fracture of Engineering Material & Structures*, Vol.11, No.25, 2002, pp. 1095-1102.
- [11] <http://www.airmichelin.com/databook.html>: Aircraft tire engineering data, MICHLIN

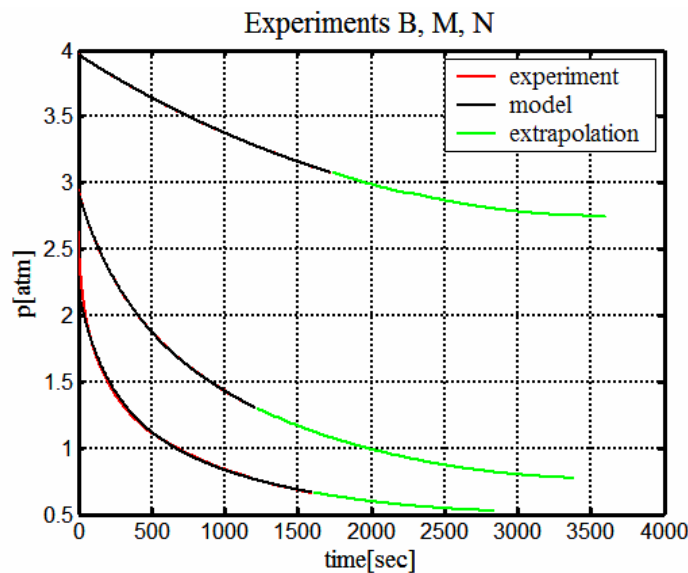


Figure 6 - $p(t)$ profile. Note that there are two lines representing the experimental data and the model prediction, in addition to the extrapolation line.